BEAMSTRAHLUNG AND PAIR PRODUCTION UNDER IP ABERRATIONS AT THE FCC-ee*

V. Gawas†[1], F. Zimmermann, J. P. T. Salvesen, CERN, Geneva, Switzerland
[1] also at University of Geneva, Geneva, Switzerland

Abstract

Beamstrahlung and secondary pair production are relevant sources of backgrounds but can also be exploited as potential tuning signals at the FCC-ee. They depend on possible interaction point (IP) optics errors and on general beam–beam conditions. Using GUINEA-PIG, we simulate beamstrahlung photons, and pair production through Breit–Wheeler, Bethe–Heitler, and Landau–Lifshitz processes and analyse the spectra, emitted power, and pair count for different sets of IP aberrations, including waist shift, vertical dispersion, and transverse coupling. The resulting photon and pair energy–angle distributions are examined, where comparisons with analytical expectations allow for consistency checks. We also compare GUINEA-PIG beamstrahlung predictions with multi-turn results delivered by the newly adopted code Xsuite, for a further benchmarking of Xsuite's beam-beam simulation package. Our study sheds light on possible beamstrahlung-related signals at the FCC-ee, including electron-positron pair production, and their dependence on the quality of the IP optics tuning.

INTRODUCTION

At future high-luminosity electron–positron colliders such as the FCC-ee, beam–beam collisions at the interaction point (IP) give rise to intense electromagnetic fields that significantly affect the properties of the colliding beams. One of the most prominent consequences is beamstrahlung, namely the emission of synchrotron-like radiation by beam particles in the field of the opposing bunch [1,2]. Together with beamstrahlung, the strong beam-beam fields also lead to the generation of secondary particles through incoherent processes such as Breit–Wheeler, Bethe–Heitler, and Landau–Lifshitz pair production [3, 4]. While these effects constitute important sources of detector background [5], they also carry detailed information on the beam–beam configuration and on the quality of the IP optics.

Beamstrahlung emission and incoherent pair production are sensitive to the local beam sizes and overlap conditions at the IP, especially with FCC-ee's flat beams. Consequently, residual optics aberrations resulting in luminosity degradation, such as waist shifts, vertical dispersion, and transverse coupling can induce measurable variations in the photon emission rates, their energy spectra, and angular distributions, as well as in the production of secondary electron–positron pairs [6–9]. This sensitivity makes beamstrahlung-related observables promising candidates for non-invasive beam diagnostics and for luminosity optimisation strategies at the FCC-ee.

Table 1: Key FCC-ee Beam Parameters for Z and $t\bar{t}$ Energies.

Parameter	Z	$t\bar{t}$
Number of bunches n_b	11200	64
Bunch intensity N	2.16×10^{11}	1.48×10^{11}
Horiz. emittance ε_x [nm]	0.70	1.51
Vert. emittance ε_y [pm]	1.9	1.36
β_x^* [m]	0.11	0.90
β_y^* [mm]	0.7	1.4
Bunch length σ_z [mm]	5.57	1.91
BS bunch length $\sigma_{z,\mathrm{BS}}$ [mm]	15.6	2.32
BS Energy spread σ_δ	1.16×10^{-3}	1.92×10^{-3}
Half-crossing angle ϕ [mrad]	15	15

However, a systematic comparison of the relative impact of different IP aberrations on both beamstrahlung emission and incoherent pair production, as well as their potential use as tuning observables, remains limited. While centroid offsets also constitute IP aberrations, their impact is treated separately [10]. In this study, we investigate the impact of selected IP aberrations on beamstrahlung and incoherent pair production using GUINEA-PIG [11–13], a well-established beam–beam simulation code. We focus on vertical waist shifts and dispersion, which are among the dominant contributors to luminosity degradation and are relevant for operation with low vertical emittance [14]. Transverse coupling, which requires multiturn simulations is not studied here, but is addressed in a complementary study based on Xsuite [14], which also includes beamstrahlung, but not yet any pair production.

Simulations are performed with GUINEA-PIG [13] using 10^6 macroparticles per beam and the beamstrahlung-broadened bunch length $\sigma_{z,\mathrm{BS}}$ as input. We study two FCC-ee working points: the Z pole ($E_{\mathrm{beam}} = 45.6\,\mathrm{GeV}$) and the $t\bar{t}$ threshold ($E_{\mathrm{beam}} = 182.5\,\mathrm{GeV}$). The key parameters for both working points are listed in Table 1 [7].

Only one IP aberration is applied at a time, while all other parameters are kept at their nominal values. The vertical waist shift Δs is scanned over the range $[-1000, +1000]$ µm, and the vertical dispersion D_y^* over $[-100, +100]$ µm. The beamstrahlung power is evaluated independently for each beam every second.

BEAMSTRAHLUNG SCANS

Beamstrahlung provides a direct probe of the electromagnetic fields generated during the beam-beam collision

* This work was supported by the Swiss CHART programme.
† vaibhavi.gawas@cern.ch

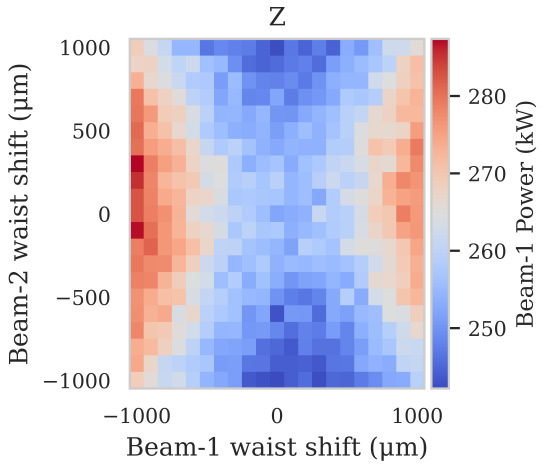

Figure 1: Beamstrahlung power as a function of vertical waist shift Δs at the Z working point.

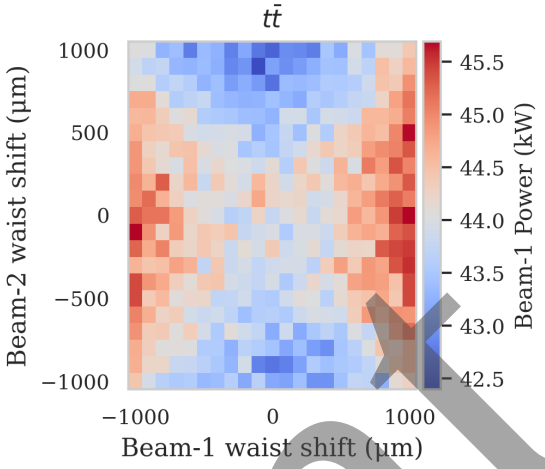

Figure 2: Beamstrahlung power as a function of waist shift at the $t\bar{t}$ working point.

and, therefore, is intrinsically sensitive to changes in the transverse beam parameters at the IP. In the flat-beam limit ($\sigma_x^* \gg \sigma_y^*$), the beam-beam force simplifies considerably. For $|y_1| \ll \sigma_{y,2}^*$, where the subindices 1 and 2 refer to the two beams, the force experienced by a particle of beam 1 scales as $F_{y,1} \propto N y_1/(\sigma_{z,2}^* \sigma_{x,2}^* \sigma_{y,2}^*)$. In linear approximation, the average beamstrahlung-induced energy loss for beam 1 scales as [15]

$$\langle \Delta E_1 \rangle \propto \sigma_{z,2}^* \langle F_{y,1}^2 \rangle \propto \frac{N^2}{\sigma_{z,2}^* \sigma_{x,2}^{*2}} \frac{\sigma_{y,1}^{*2}}{\sigma_{y,2}^{*2}}. \quad (1)$$

Therefore, an increase in the size of beam 2, e.g., in $\sigma_{y,2}^*$, reduces the beamstrahlung power emitted by beam 1, while an increase in the vertical size of beam 1 enhances the power emitted by beam 1, which is sampling stronger focusing fields from the denser opposing bunch. This sign asymmetry is evident in the scans of IP waist and IP dispersion.

Figures 1 and 2 present the beamstrahlung power simulated by GUINEA-PIG as a function of vertical waist shift Δs for the Z and $t\bar{t}$ working points respectively. Average of beamstrahlung energy over 5-10 bunch crossings is scaled to get the power values. The power of beam 1 decreases when the waist of beam 2 is shifted, and increases when the waist of beam 1 itself is shifted. The curves are therefore antisymmetric about $\Delta s = 0$.

Figure 3 shows the beamstrahlung power of one beam as a function of IP vertical dispersion D_y^* at the Z working point. The same sign asymmetry between the two beams is observed as in the waist shift case. The relatively modest variation of beamstrahlung power with waist shift, compared with vertical dispersion, can be understood from the fact that the beam size contribution from a waist shift grows only quadratically in Δs, so that beam–beam and hourglass effects can partially mitigate the naive geometric prediction at large waist offsets [16, 17]. The dispersion curves exhibit a markedly sharper dependence on aberration strength and significantly lower noise than the waist shift results. This contrast has a clear analytical origin. For

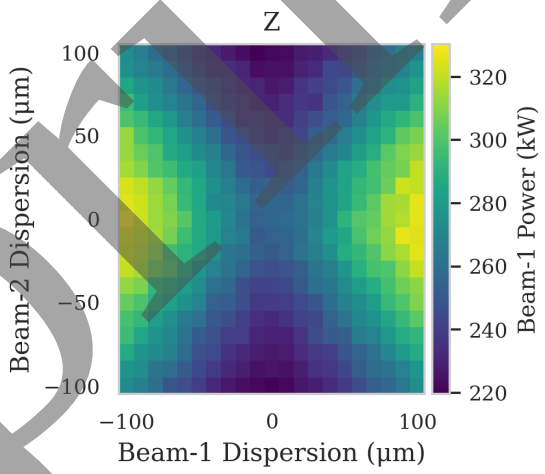

Figure 3: Beamstrahlung power as a function of vertical dispersion at the Z working point.

a waist shift Δs, the effective vertical beam size grows as $\Delta\sigma_y^*/\sigma_y^* \approx (1/2)\,(\Delta s/\beta_y^*)^2$, which is quadratic in Δs, keeping the fractional beam size increase $\Delta\sigma_y^*/\sigma_y^*$ small over the range studied. For vertical dispersion, the additional beam size contribution is $\Delta\sigma_y^*/\sigma_y^* \approx (D_y^*\sigma_\delta)^2/(2\sigma_y^{*2})$, which is also quadratic in D_y^* for small $D_y^*\sigma_\delta/\sigma_y^*$, but with a coefficient enhanced by the factor $\sigma_\delta^2/\sigma_y^{*2}$. At the FCC-ee Z pole, where $\sigma_y^* \sim 40\,\text{nm}$ and $\sigma_\delta \sim 10^{-3}$, even modest values of D_y^* produce a fractional beam size increase substantially larger than that from a comparable waist shift, yielding considerably tighter beamstrahlung-based tolerances on vertical dispersion.

INCOHERENT PAIR PRODUCTION

In addition to photon emission, beam–beam interactions at the IPs lead to the production of secondary electron–positron pairs through incoherent processes, namely Breit–Wheeler (BW), Bethe–Heitler (BH), and Landau–Lifshitz (LL) interactions [3, 4]. The pair production rates depend on both

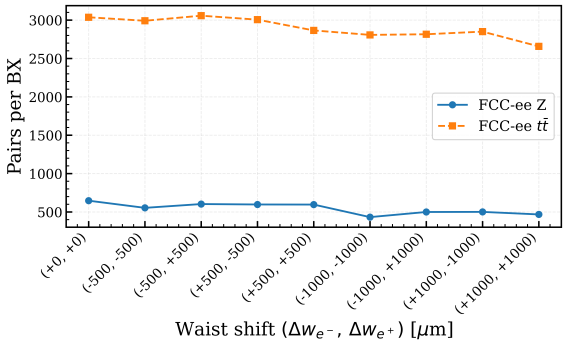

Figure 4: Total incoherent pair yield per bunch crossing as a function of vertical waist shift at the Z and $t\bar{t}$

the beamstrahlung photon spectrum and the collective electromagnetic fields of the colliding bunches. We analyse the total pair yield as a function of vertical waist shift and vertical dispersion for the Z and $t\bar{t}$ working points.

Figure 4 shows the total incoherent pair production yield per bunch crossing as a function of vertical waist shift Δs.

The total pair production yield shows a weak dependence on vertical waist shift, consistent with the modest variations observed in beamstrahlung power over the $\pm 1000\,\mu$m scan range. This follows from the fact that pair production rates are driven primarily by the beamstrahlung photon flux.

In contrast to the waist shift case, pair production exhibits a substantially stronger sensitivity to vertical dispersion as shown in Fig. 5, consistent with the enhanced beamstrahlung photon flux. These results reinforce the conclusion that vertical dispersion is the dominant aberration for IP performance degradation, and that beamstrahlung and pair production observables are sensitive diagnostics for this class of error.

COMPARISON WITH XSUITE

To validate the modelling of beamstrahlung in GUINEA-PIG, we compare its predictions with multi-turn strong-strong beam–beam simulations performed using Xsuite [18]. All comparisons are carried out at the $t\bar{t}$ working point, where beamstrahlung is strongest and the signal-to-noise ratio is most favourable.

Figure 6 shows the beamstrahlung power as a function of vertical waist shift. The two codes show agreement at the

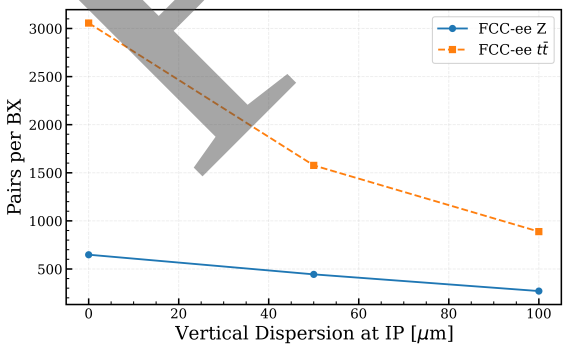

Figure 5: Total incoherent pair production yield per bunch crossing as a function of vertical dispersion D_y^* at the Z and $t\bar{t}$.

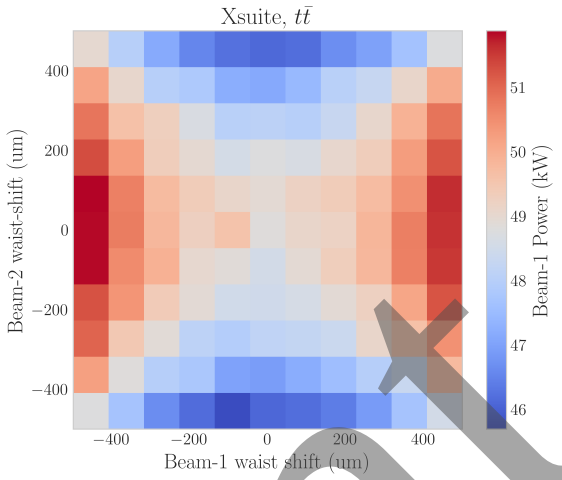

Figure 6: Beamstrahlung power of the electron beam as a function of vertical waist shift Δs at $t\bar{t}$ in Xsuite (strong-strong, averaged over turns 800–1000).

10–20% level across the ± 500 μm scan range, with both reproducing the same qualitative dependence on waist shift. The shapes of the two curves are in good correspondence, indicating that the beam size dependence is correctly captured in both frameworks.

The level of agreement is consistent with the differences expected from the distinct numerical implementations: GUINEA-PIG treats the beam–beam interaction as a single-pass event with a fixed phase-space distribution and particle in cell calculations, whereas Xsuite propagates the full linear multiturn dynamics including synchrotron radiation damping and quantum excitation, and soft-gaussian based beam-beam dynamics.

CONCLUSION

We investigated the sensitivity of beamstrahlung emission and incoherent pair production to residual vertical optics aberrations at the FCC-ee IP, using GUINEA-PIG simulations at the Z pole and $t\bar{t}$ working points. Vertical dispersion is found to have a significantly stronger impact on beamstrahlung power and pair production than vertical waist shifts, owing to the linear vs. quadratic dependence of the respective beam size contributions on the aberration strength. The sharper and cleaner variation of beamstrahlung power with dispersion strength suggests that beamstrahlung power measurements could serve as a sensitive and practical feedback signal for tuning IP dispersion knobs non-invasively. The sign asymmetry of the beamstrahlung response between the two beams, observed consistently across all scans, is physically understood as a consequence of the directional nature of the beam–beam interaction and provides a built-in consistency check for simulation and measurement alike. A comparison of GUINEA-PIG single-pass results with multi-turn strong-strong Xsuite simulations at $t\bar{t}$ shows agreement at the 10–20% level.

REFERENCES

[1] P. Chen, "Quantum Beamstrahlung from Gaussian Bunches", in *Workshop on New Developments in Particle Acceleration Techniques*, Orsay, France, Jun.-Jul. 1987.

[2] P. Chen, "Disruption Effects from the Collision of Quasi-Flat Beams", in *Proc. PAC'93*, Washington D.C., USA, Mar. 1993, pp. 617–620.

[3] VN. Baier, VS. Fadin, VA. Khoze, and EA. Kuraev, "Inelastic processes in high energy quantum electrodynamics", *Phys. Rep.*, vol. 78, no. 3, pp. 293–393, 1981. doi:https://doi.org/10.1016/0370-1573(81)90140-X

[4] C. Rimbault, P. Bambade, K. Mönig, and D. Schulte, "Incoherent pair generation in a beam-beam interaction simulation", *Phys. Rev. Spec. Top. Accel. Beams*, vol. 9, no. 3, p. 034402, Mar. 2006. doi:10.1103/PhysRevSTAB.9.034402

[5] D. Schulte, Background at Future Linear Colliders, 1999, https://cds.cern.ch/record/419592

[6] M. Benedikt *et al.*, "FCC-ee: the lepton collider: Future Circular Collider conceptual design report volume 2", *Eur. Phys. J. Spec. Top.*, vol. 228, pp. 261–623, 2018. doi:10.1140/epjst/e2019-900045-4

[7] B. Auchmann *et al.*, "FCC Midterm Report", CERN, Geneva, Switzerland, Rep., Feb. 2024. doi:10.17181/zh1gz-52t41

[8] P. Bambade, R. Erickson, W. A. Koska, W. Kozanecki, N. Phinney, and S. R. Wagner, "Observation of beam-beam deflections at the interaction point of the SLAC linear collider", *Phys. Rev. Lett.*, vol. 62, no. 25, pp. 2949–2952, Jun. 1989. doi:10.1103/PhysRevLett.62.2949

[9] M. G. Minty and F. Zimmermann, *Measurement and Control of Charged Particle Beams*. Heidelberg, Germany: Springer, 2003. doi:10.1007/978-3-662-08581-3

[10] J. Salvesen, F. Zimmermann, and P. Burrows, "First studies on error mitigation by interaction point fast feedback systems for FCC-ee", in *Proc. IPAC'24*, Nashville, TN, USA, pp. 3322–3325, Jul. 2024. doi:10.18429/JACoW-IPAC2024-THPG31

[11] D. Schulte, "Study of Electromagnetic and Hadronic Background in the Interaction Region of the TESLA Collider", Ph.D. thesis, Hamburg U., 1997.

[12] D. Schulte, Beam-Beam Simulations with GUINEA-PIG, 1998, https://cds.cern.ch/record/382453

[13] Guinea-pig++, 2024, https://abpcomputing.web.cern.ch/codes/codes_pages/Guinea-Pig/

[14] V. Gawas, X. Buffat, P. Kicsiny, and F. Zimmermann, "Effect of FCC-ee Optics Errors in Collision Simulated by Xsuite", presented at IPAC'26, Deauville, France, May 2026, paper WEP5045, this conference,

[15] K. Yokoya and P. Chen, "Beam-beam phenomena in linear colliders", in *Frontiers of Particle Beams: Intensity Limitations*, pp. 415–445, 1992.

[16] M. A. Furman, "Hourglass effects for asymmetric colliders", in *Proc. IEEE PAC 1991*, San Francisco, CA, USA, May 1991, pp. 422–424. doi:10.1109/PAC.1991.164321

[17] M. Venturini and W. Kozanecki, "The hourglass effect and the measurement of the transverse size of colliding beams by luminosity scans", in *Proc. PAC 2001*, Chicago, IL, USA, Jun. 2001, p. 3573.

[18] G. Iadarola *et al.*, "Xsuite: An Integrated Beam Physics Simulation Framework", in *Proc. HB'23*, Geneva, Switzerland, Oct. 2023, pp. 73–80. doi:10.18429/JACoW-HB2023-TUA2I1